

# Study on Electrochemical Processes of NiO Model Electrode during the First Lithiation/delithiation Cycle via Electrochemical Impedance Spectroscopy

*Lei Wang, Haixia Wu\* and Shouwu Guo\**

Department of Electronic Engineering, School of Electronic Information and Electrical Engineering, Shanghai Jiao Tong University, Shanghai 200240, P. R. China

\*E-mail: [haixiawu@sjtu.edu.cn](mailto:haixiawu@sjtu.edu.cn), [swguo@sjtu.edu.cn](mailto:swguo@sjtu.edu.cn)

*Received:* 9 July 2018 / *Accepted:* 10 August 2018 / *Published:* 5 November 2018

---

Transition metal oxides (TMOs) have been researched as active electrode materials for Li-ion batteries for over 20 years owing to their large specific capacity based on conversion reactions rather than intercalation/deintercalation mechanism. Here, NiO was chosen not only as a representative among those TMOs but also as a model electrode material to fundamentally study its electrochemical processes during the first lithiation/delithiation cycle via electrochemical impedance spectroscopy (EIS). The NiO model electrode was constructed by electrodepositing a pure NiO film on the surface of the copper foil and directly served as a working electrode in Li-ion half cells without any other additives. These cells were stopped at certain states in the first lithiation/delithiation cycle and ready for the EIS test. Interestingly, other two semicircles were found in Nyquist plots, which were ascribed to NiO and structure transformation besides the normal two semicircles related to solid electrolyte interphase (SEI) and the interface between NiO and electrolyte. Furthermore, bounded diffusion was more suitable than semi-infinite diffusion to explain  $\text{Li}^+$  diffusion process in conversion-type electrodes. Thus, a new fitting circuit was proposed and the electrochemical processes of the NiO model electrode were studied quantitatively according to fitted data.

---

**Keywords:** NiO, EIS, Li-ion battery, fitting circuit

## 1. INTRODUCTION

Transition metal oxides (TMOs) such as  $\text{Mn}_3\text{O}_4$ ,  $\text{Fe}_3\text{O}_4$ ,  $\text{Co}_3\text{O}_4$ , NiO,  $\text{Cu}_2\text{O}$  have been increasingly studied for over 20 years as active electrode materials because of their high theoretical capacity and low cost [1-3]. Various methods including in situ X-ray, in situ transmission electron microscopy, and thermodynamic analysis have been employed to elucidate their electrochemical

processes during cycling [4-6]. Different from the intercalation/deintercalation mechanism, they undergo conversion reactions with the reduction and oxidation of metal particles. Here, NiO was chosen not only as a representative of these TMOs but also as a model electrode material to illustrate its electrochemical processes during the first lithiation/delithiation cycle.

In order to better understand the electrochemical processes and conversion reactions mechanism of NiO during the first lithiation/delithiation cycle, electrochemical impedance spectroscopy (EIS) was utilized and clearly analyzed. EIS is a powerful method and frequently used to reveal the electrochemical processes of lithium-ion battery. For the past two decades, many EIS researchers have dedicated to studying the solid electrolyte interphase (SEI) [7], electronic and ionic transport properties [8] of the cathodes and anodes in Li-ion batteries, which were based on intercalation/deintercalation mechanism. Nevertheless, the same interpretation has also been used to describe the processes in Li-ion batteries based on conversion reactions mechanism, which often led to misfit especially within the low-frequency region [9]. At the same time, because of its intrinsic poor electrical conductivity, aggregation and large volume change during cycling, pure NiO has to be modified to improve its cycling stability and rate performance such as complexing with Ni [10-12], graphene [13, 14], or carbon nanotubes [15] in consideration of application requirements. Conductive agents and binders including acetylene black, carbon nanotubes, polyvinylidene fluoride (PVDF), polytetrafluoroethylene (PTFE) are usually needed to improve its conductivity and prevent against falling off from current collectors. These additives introduce a lot of interference to the basic research of electrochemical processes, as well as bring great difficulties to analysis processes. However, little effort has been devoted to exploring the electrochemical behavior of pure NiO or model electrode in the Li-ion batteries without such additives as mentioned above.

Therefore, in this study, we designed a kind of NiO model electrode which was deposited on the surface of copper foil by electroplating without any other additives. Then we assembled it into a coin Li-ion cell. After that, we chose a new fitting circuit with a different diffused element called T element which is referred to bounded diffusion (comparable to W element which is referred to semi-infinite diffusion) to study the electrochemical processes according to the measured EIS data. And the evolution of NiO electrode in the Li-ion batteries during the first cycle was clearly disclosed based on the new and perfect fitting.

## 2. EXPERIMENTAL

A layer of NiO film on the surface of the copper foil was prepared by a simple electroplating method and heat treatment. In detail, an electroplating device was constructed with a piece of acid cleaned copper foil (40 mm\*120 mm) as the working electrode, a piece of nickel foam (42 mm\*140 mm) as the counter and reference electrode respectively, and 250 mL 0.25 mol/L Ni(NO<sub>3</sub>)<sub>2</sub> ethanol aqueous solution (1 : 1, volume ratio, pH = 3.5) as the plating solution. Between the electrodes, voltage -1.6 V was added for 2 hours while the plating solution was kept constantly at 30 °C. After electroplating, the copper foil covered with a layer of light green Ni(OH)<sub>2</sub> was carefully washed by deionized water several times and vacuum dried at 60 °C for 2 hours. And then the product was treated

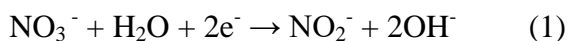
at 350 °C in a flowing Ar atmosphere for 3 hours for completely converting it to dark NiO. The NiO electroplated copper foil was acted as the working electrode directly in the Li-ion batteries where copper foil could collect current and NiO participated in electrochemical reactions with Li foil as the counter and reference electrode, a Celgard 2025 membrane as the separator and 1 M LiPF<sub>6</sub> in a 1: 1 mixture solution of ethylene carbonate and diethyl carbonate (EC/DEC) as the electrolyte.

Ultra 55 field emission-scanning electron microscopic (FE-SEM) (Zeiss, Germany) under a working voltage of 10 kV was used to examine the morphology of the electrode and energy dispersive spectroscopy (EDS) was attached to measure the element types and contents. D8 ADVANCE diffractometer (Bruker, Germany) was used to capture the X-ray diffraction (XRD) patterns of Ni(OH)<sub>2</sub> and NiO which were peeled off from the copper foil.

In order to illustrate the evolution of the NiO model electrode during the first cycle, cyclic voltammetry (CV) curve which was conducted between 0.01 V to 3 V at a scanning rate of 5 mV s<sup>-1</sup> by an electrochemical working station (PGSTAT 302N) (Metrohm, Switzerland), then 6 potential including pristine (before cycled), D-1V (discharged state of 1 V), D-0.01V (discharged state of 0.01 V), C-1V (charged state of 1 V), C-2V (charged state of 2 V), and C-3V (charged state of 3V) were chosen to be studied. Then the as-assembled Li-ion cells were discharged to 1 V, discharged to 0.01 V or continued to be charged to 1 V, 2 V, or 3 V by LAND CT2001A (Wuhan, China) at a current density of 0.1 A g<sup>-1</sup> and stood by for 2 hours to reach a steady voltage respectively. Then, each cell was conducted by PGSTAT 302N controlled by Nova 1.11 software to obtain EIS in which the perturbation voltage was 10 mV and the frequency range varied from 100 KHz to 100 mHz. After that, the EIS was analyzed by a program attached in Nova software with the new fitting circuit.

### 3. RESULTS AND DISCUSSION

The NiO model electrode was prepared based on three chemical reactions. When the voltage of -1.6 V was applied, OH<sup>-</sup> was produced near the working electrode, which led to a small alkaline area even though the solution pH value was 3.5. Meanwhile, some Ni(OH)<sub>2</sub> seed crystals were formed in this area, and because of the low density of the Ni(OH)<sub>2</sub> seed, they preferred to deposit on the heterogeneous surface of the copper foil. These seed crystals then grew into a thin light green Ni(OH)<sub>2</sub> film for 2 hours [16] as shown in Figure 1a. After drying, the Ni(OH)<sub>2</sub> electrode was put into a tube furnace and changed into black NiO (Figure 1a) under 350 °C based on a decomposition reaction. The three chemical reactions were simply written in three equations below:



The model electrode has a rough surface and NiO is partially covering the copper foil from the SEM image (Figure 1b). The XRD patterns (Figure 1c) show that the two materials have totally different diffraction peaks. The 2θ values of 33.665°, 38.957°, 60.897° can be indexed to (110), (200), (301) diffraction planes of Ni(OH)<sub>2</sub>. And the 2θ values of 37.248°, 43.275°, 62.878° can be indexed to (111), (200), (220) diffraction planes of cubic NiO. The diffraction peaks are a little broad because of

the low degree of crystallinity of Ni(OH)<sub>2</sub> and NiO particles.

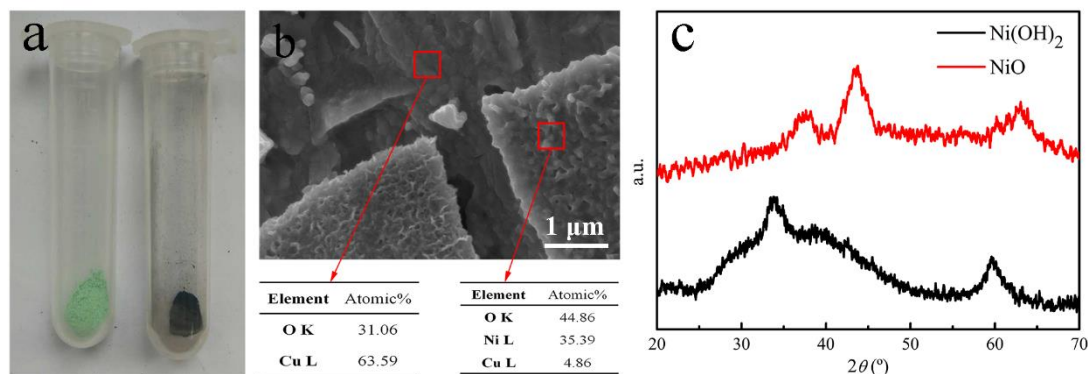


**Figure 1.** (a) Photographs of Ni(OH)<sub>2</sub> (left) and NiO (right) samples peeled from the copper foil; (b) SEM image and EDS data of electroplated copper foil covered by NiO; (c) XRD patterns of Ni(OH)<sub>2</sub> and NiO samples.

Cyclic voltammetry was done to illustrate the evolution of the NiO model electrode during the first cycle. From the CV plot shown in Figure 2, the NiO electrode has a cathodic peak around 0.5 V corresponding to the formation of Ni and solid electrolyte interphase (SEI) film and two anodic peaks around 1.7 V and 2.23 V corresponding to the decomposition of SEI film and the formation of NiO [17]. To show how the electrode changes before and after these chemical reactions happened, six points were chosen almost equidistantly and highlighted by red dots on the CV curve.

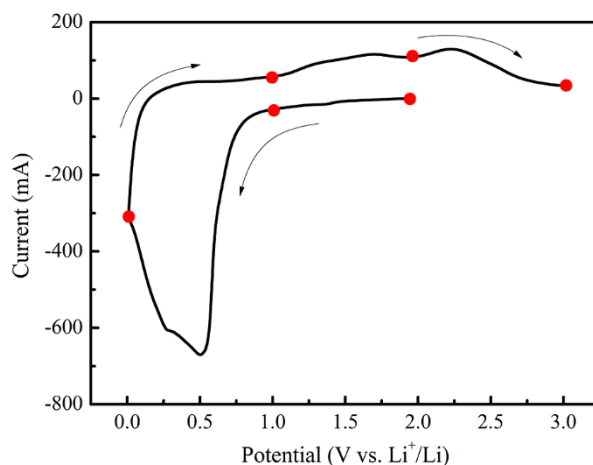


**Figure 2.** A cyclic voltammetry curve of NiO model electrode during the first cycle. It was discharged from open circuit potential to 0.01 V and then charged to 3 V as indicated by arrows. Six typical potentials were highlighted and selected to study the electrochemical process of NiO model electrode.

To explicitly explain why this new fitting circuit is used and how it works, D-0.01V was selected as a representative. A typical process of NiO electrode reactions around this potential during AC impedance test is illustrated in Figure 3a. First, the Li<sup>+</sup> in the liquid electrolyte travels through the SEI film and arrives at the surface of NiO film. Meanwhile, the e<sup>-</sup> from the current collector arrives at

the same place and gives rise to a electrochemical reaction ( $\text{NiO} + 2\text{Li}^+ + 2\text{e}^- \rightarrow \text{Ni} + \text{Li}_2\text{O}$ ) [18]. A Similar process can be found in the graphite electrode, where  $\text{Li}^+$  migrates through SEI film and then intercalates into graphite, accompanied by charge transfer at its surface [19]. This place is so called the chemical reaction site. Based on this understanding, a new fitting circuit was put forward to comply with this process.

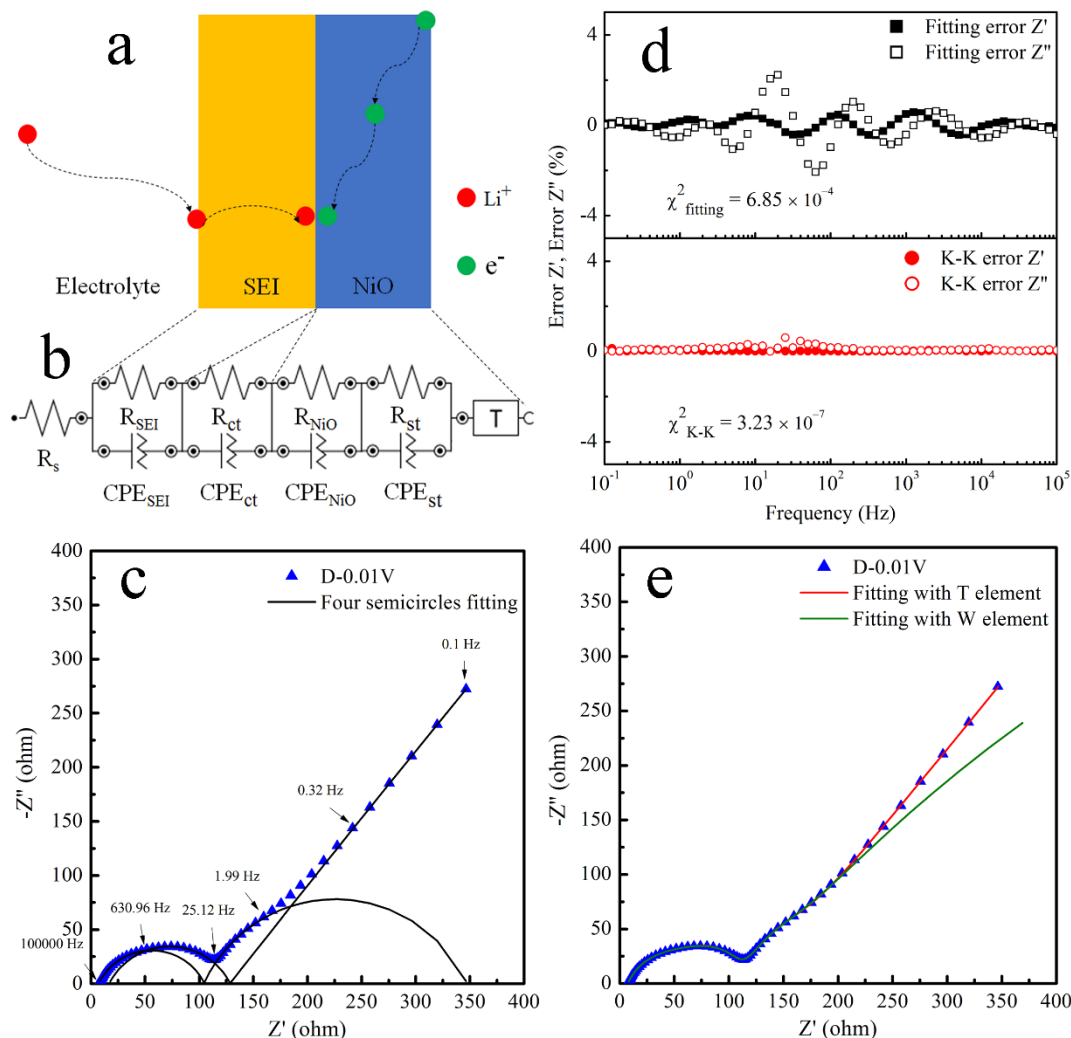


**Figure 3.** EIS fitting of battery D-0.01V as a representative: (a) Scheme of a typical electrochemical process in the NiO electrode; (b) a fitting circuit based on the understanding of the electrochemical process used to fit the EIS; (c) obtained Nyquist plot with four indicated semicircles; (d) the error plots of fitted data and K-K test; (e) comparison of fitting with T and W element without any changes of other elements.

In theory, the structure of a cell can be explained by numerous elements such as resistors (R), capacitors (C) and inductors (L), which can form a very complex structure in series or parallel. But many elements can be merged into a relatively simple structure due to their similar time constants [20]. As is showed in Figure 3b, a new fitting circuit composed of one R, four parallel RC circuits, one T in series corresponding to four semicircles and one straight line in the Nyquist plot (Figure 3c) is applied

to fit the cell D-0.01V to reveal its structure. In most cases, capacitors are replaced by constant phase angle elements (CPE) due to the capacitance dispersion effect caused by porous, rough or absorbed electrodes [21]. The impedance of the CPE is

$$Z_{CPE} = \frac{1}{Y_0(j\omega)^n},$$

where  $Y_0$  is the parameter related to the capacitance of the electrode ( $F \text{ s}^{n-1} \text{ cm}^2$ ) and  $n$  is the constant phase exponent ( $0 \leq n \leq 1$ ). The first semicircle located from 100000 Hz to 630.96 Hz is related with the SEI film in which  $R_{SEI}$  and  $CPE_{SEI}$  are the resistance and capacitance of the SEI film. The second semicircle located from 630.96 Hz to 25.12 Hz is related with the NiO in which  $R_{NiO}$  and  $CPE_{NiO}$  are the resistance and polarization capacitance of NiO. Here, because  $e^-$  is difficult to move through NiO, the time constant  $RC$  of the second semicircle is big enough to respond in the selected frequency region. If the electrical conductivity of the electrode material is very good or improved by mixing with conductive agents, its resistance will be too small to be recorded [22], that means pure NiO in the Li-ion batteries without such additives can avoid such interference. The third semicircle located from 25.12 Hz to 1.99 Hz is in connection with the interface exchange process in which  $R_{ct}$  is the charge transfer resistance and  $CPE_{ct}$  is the capacitance on the surface of NiO, which is often used to analyze the kinetic properties in Li-ion batteries [7, 8, 23]. The fourth circle located from 0.32 Hz to 0.1 Hz is the result of the transformation between NiO and Ni as a consequence of the conversion reactions or formation of new phases, which is also mentioned in other kinds of literatures. For example, Evgenij et al. found that phase nucleation processes could be presented after 700 s (about 1.4 mHz) due to the rate-limited growth of lithium-rich phase [24]. They also found that phase change of  $LiNiO_2$  material could be detected among such a low frequency (to 0.2 mHz) [25]. NiO belongs to a cubic system with  $a = 4.1771 \text{ \AA}$  from PDF#47-1049 in this paper which is very different from whatever cubic with  $a = 3.5238 \text{ \AA}$  or hexagonal with  $a = b = 2.6515 \text{ \AA}$ ,  $c = 4.343 \text{ \AA}$  Ni. Even they are different substances with different electronic structures. This structure transformation can be displayed at a very low frequency, usually below 0.01 Hz. Fortunately, almost 7 points can be ascribed to this structure transformation of NiO model electrode at a low frequency from 0.32 Hz to 0.1 Hz. And because the  $R_{st}$  is too large, about 1.47 k $\Omega$  in D-0.01V, the fourth semicircle has a large diameter that equals to  $R_{st}$  and seems like a straight line within this region. T element represents bounded diffusion of  $Li^+$  in the NiO model material, which is well different from semi-infinite diffusion in the layered compounds. The expression of T is

$$Z_T = \frac{1}{Y_0\sqrt{j\omega}} \coth(B\sqrt{j\omega}),$$

in which

$$Y_0 = \frac{nFC_s\sqrt{D}}{Z_F^0\gamma|I_F|}$$

and

$$B = \frac{l}{\sqrt{D}},$$

where  $n$  is the number of electrons exchanged in the process,  $F$  is the Faraday constant,  $C_s$  is the surface concentration of the species,  $D$  is the diffusion coefficient ( $\text{cm}^2 \text{ s}^{-1}$ ),  $Z_F^0$  is the Faraday impedance,  $\gamma$  is the reaction order,  $I_F$  is the Faraday current density,  $l$  is the bounded layer thickness

(m). The T element is utilized in the fitting circuit and fitted well with the recorded data, which indicates that the limited  $\text{Li}^+$  diffusion distance is similar to the  $\text{Li}^+$  radius.

Figure 3d is the fitting error and Kramers-Kronig (K-K) test error of the acquired EIS data of cell D-0.01V. It shows that both errors are around 0 and below 3%. The chi-square of the fitted data is  $6.85 \times 10^{-4}$ , elucidating that fitting circuit is probably reasonable. The chi-square of the K-K test is  $3.23 \times 10^{-7}$ , which illustrates that the acquired EIS data obeys the principle of the EIS test. To demonstrate the reasonability of the T element, W element was also taken into this circuit for examination and comparison without any changes of other elements. As shown in Figure 3e, these two elements don't influence the conformity between the acquired data and fitted data within the high and mediate frequency region. Nevertheless, they have an obvious difference in the low-frequency region. The T element shows well in accordance with the acquired data but the W element shows an obvious deviation, resulting in a worse fitting. This further demonstrates that  $\text{Li}^+$  follows bounded diffusion rather than semi-infinite diffusion.

Applying this fitting circuit, the Nyquist plots (Figure 4a) and Bode phase plots (Figure 4b) of batteries in other potential are also fitted well with their variances of fitting  $\chi^2$  generally below  $10^{-3}$ , which indicates that this fitting circuit is probably right. As is showed in the Nyquist plots, they have several semicircles within high and middle-frequency regions, and a line within low-frequency regions. Whereas, note that within an even lower frequency region around 0.1 Hz, it is a small part of a large semicircle caused by structure transformation. As for Bode phase plots, each RC parallel circuits will form a peak, corresponding to the semicircles in the Nyquist plots. Note that each Bode phase plot is also fitted well by this new circuit.

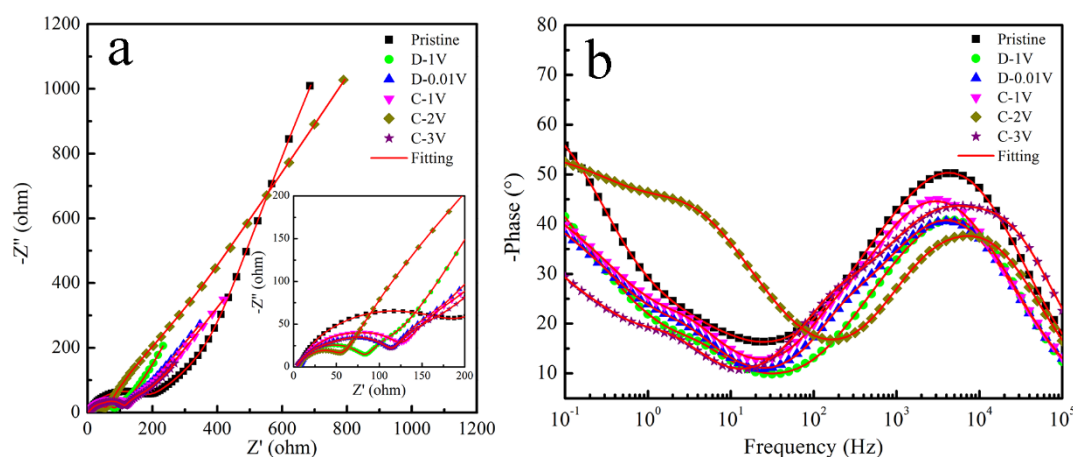


**Figure 4.** Nyquist plots (a) and Bode phase plots (b) of the batteries under different potential. Each curve is fitted by the same fitting circuit. Inset of a is amplified Nyquist plots.

**Table 1.** Fitted data of NiO Li-ion batteries under different potential states.

Batteries	$R_s/\Omega$	$R_{SEI}/\Omega$	$R_{NiO}/\Omega$	$R_{ct}/\Omega$	$R_{st}/\Omega$	B/s	$\chi^2/10^{-4}$
Pristine	6.67	37.4	133	223	11.3 k	0.863	4.48
D-1V	6.74	32.6	39.1	7.46	1.04 k	0.785	9.47
D-0.01V	7.63	63.6	34.1	14.4	1.47 k	0.967	6.85
C-1V	6.69	90.7	19.8	19.9	4.38 k	1.06	9.15
C-2V	6	8.94	38.3	78.7	81 k	0.822	3.26
C-3V	3.69	3.38	105.4	42	227	0.726	6.47

The fitted data are extracted from the fitting circuits and summarized in Table 1 in order to study the evolution of electrochemical processes of pure NiO electrode during the first lithiation/delithiation cycle. To clearly observe the evolution of  $R_s$ ,  $R_{SEI}$ ,  $R_{NiO}$ ,  $R_{ct}$ , and  $R_{st}$ , Figure 5 is displayed below. From Figure 5a,  $R_s$  which represents the resistance of the electrolyte is nearly the same in the six batteries, which is in good agreement with the actual situations, as the electrolyte is an overdose and the product of electrode reactions could hardly influence the composition as well as the conductivity of the electrolyte. Surprisingly, SEI film had already formed before the cathodic reaction potential at about 0.5 V. The SEI film in the pristine batteries might be on account of the spontaneous reactions on NiO during the aging process. To demonstrate the formation of SEI film before 0.5 V, the CV plot is enlarged in Figure 6a. Obviously, a broad peak around 1.64 V and a small peak around 1.34 V are found, which could be caused by different electrolyte decomposition reactions happened step-by-step. SEM image of Figure 6b further demonstrated that the NiO is covered by a smooth film after discharged to 1 V, which is well different from the as-prepared rough NiO electrode in Figure 1b. The SEI film is still produced from sample D-0.01V because of the low cathodic potential and has the largest resistance from sample C-1V because it was under the low potential for the longest time even though the potential was added reversely. From half cells C-2V and C-3V, the SEI film has the lowest resistance of 8.94  $\Omega$  and 3.38  $\Omega$ , which must have something to do with the SEI film decomposition reaction at around 1.7 V. This huge SEI film decomposition reaction may induce the capacity fading when batteries are cycled for long times, which is a major concern of the native NiO as a steady SEI film is necessary in Li-ion batteries [26, 27]. The evolution of  $R_{NiO}$  shows that the pristine NiO has the largest resistance before it is cycled and decreases gradually until 19.8  $\Omega$  of C-1V that could have the maximum amount of conductive metallic Ni particles from reduced NiO. The resistance of NiO then increases and is 105.4  $\Omega$  of C-3V, which relates to the oxidation reaction of Ni at around 2.23 V. Figure 5b shows that  $R_{NiO}$  and  $R_{ct}$  have similar values and follow a similar variation tendency during the first cycle, which suggests that  $R_{ct}$  may be positively related to  $R_{NiO}$ . If  $R_{NiO}$  is reduced, the charge transfer process can be accelerated. Furthermore,  $R_{st}$  plays an important role during the first cycle because it always has the highest value in all the batteries illustrated in Figure 5c. The huge resistance of NiO electrode transformation could be detrimental to Li-ion batteries and treatments should be adopted to alleviate its harmful effects. In addition, B that is equal to  $\frac{l}{\sqrt{D}}$  from the T element is hardly changed, which indicates that the diffusion coefficient of  $Li^+$  in the NiO electrode is hardly influenced.

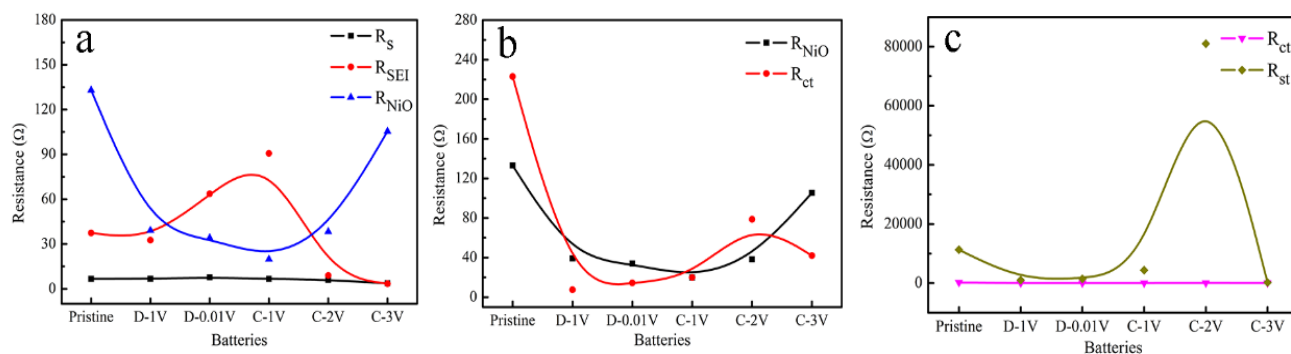


**Figure 5.** Comparison of the evolution of  $R_s$ ,  $R_{SEI}$ ,  $R_{NiO}$  (a),  $R_{NiO}$ ,  $R_{ct}$  (b),  $R_{ct}$ ,  $R_{st}$  (c) of the NiO model electrode during the first lithiation/delithiation cycle.

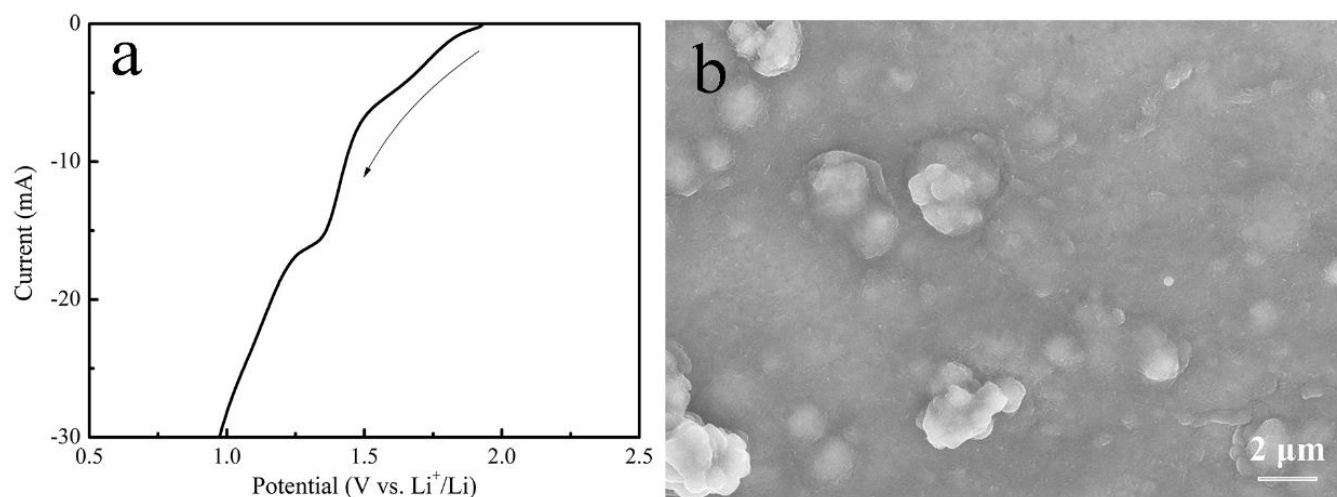


**Figure 6.** (a) Enlarged CV plot between 0.5 V and 2.5V of Figure 2; (b) SEM image of the NiO electrode after it was discharged to 1 V.

#### 4. CONCLUSIONS

To summarize, employing a new T element fitting circuit with bounded diffusion, the EIS was well fitted and interpreted to study the evolution of electrochemical processes of NiO model electrode during the first lithiation/delithiation cycle. There are some interesting and significant results: (1)  $R_s$  was hardly changed during the first cycle; (2) SEI film had already formed on the NiO before the typical cathodic reaction at around 0.5 V; (3) The formed SEI film would decompose at around 1.7 V, which indicated that the SEI film on the NiO was not steady during cycling; (4) The resistance of pristine NiO decreased obviously when the NiO was converted into Ni at low potential and increased to almost the same value after the Ni was oxidized to NiO again at around 2.23 V; (5) The  $R_{st}$  as a consequence of the repeated conversion between NiO and Ni was so large that it might damage the NiO electrode; (6) The diffusion coefficient of  $Li^+$  in NiO electrode was almost unchanged during the initial cycle.

Besides, this study shows us that T element which is related to bounded diffusion is more suitable than W element that is related to semi-infinite diffusion in the fitting circuit, which can be used as a reference to study the structural evolution of other conversion-type electrodes during the charge and discharge processes.

#### ACKNOWLEDGEMENT

We thank the National Science Foundation of China (NO. 21376148), for financial support of this work. The authors also wish to express their appreciation to the Instrumental Analysis Center of SJTU.

#### References

1. S. H. Yu, S. H. Lee, D. J. Lee, Y. E. Sung, and T. Hyeon, *Small*, 12 (2016) 2146.
2. S. H. Yu, X. Feng, N. Zhang, J. Seok, and H. D. Abruna, *Acc Chem Res*, 51 (2018) 273.
3. M. H. Oh, T. Yu, S.-H. Yu, B. Lim, K.-T. Ko, M.-G. Willinger, D.-H. Seo, B. H. Kim, M. G. Cho, J.-H. Park, K. Kang, Y.-E. Sung, N. Pinna, and T. Hyeon, *Science*, 340, (2013) 964.
4. M. A. Lowe, J. Gao, and H. D. Abruña, *J. Mater. Chem. A*, 1 (2013) 2094.
5. L. Luo, J. Wu, Q. Li, V. P. Dravid, K. R. Poepfelmeier, Q. Rao, and J. Xu, *Nanotechnology*, 27 (2016) 085402.
6. C.-X. Zu and H. Li, *Energy & Environmental Science*, 4 (2011) 2614.
7. S. S. Zhang, K. Xu, and T. R. Jow, *Electrochimica Acta*, 51 (2006) 1636.
8. Q. C. Zhuang, T. Wei, L. L. Du, Y. L. Cui, L. Fang, and S. G. Sun, *J. Phys. Chem. C*, 114 (2010) 8614.
9. G. Zhou, D. W. Wang, L. C. Yin, N. Li, F. Li, and H. M. Cheng, *ACS NANO*, 6 (2012) 3214.
10. W. Wen, J. M. Wu, and M. H. Cao, *J. Mater. Chem. A.*, 1 (2013) 3881.
11. X. Sun, W. Si, X. Liu, J. Deng, L. Xi, L. Liu, C. Yan, and O. G. Schmidt, *Nano Energy*, 9 (2014) 168.
12. J. Bell, R. Ye, K. Ahmed, C. Liu, M. Ozkan, and C. S. Ozkan, *Nano Energy*, 18 (2015) 47.
13. X. H. Huang, P. Zhang, J. B. Wu, Y. Lin, and R. Q. Guo, *Materials Letters*, 153 (2015) 102.
14. D. Qiu, G. Bu, B. Zhao, and Z. Lin, *RSC Adv.*, 5 (2015) 4385.
15. Z. Zhang, X. Zhang, X. You, M. Zhang, M. D. Walle, J. Wang, Y. Li, and Y. N. Liu, *J. Nanopart. Res.*, 18 (2016) 247.
16. M. Wohlfahrt-Mehrens, R. Oesten, P. Wilde, and R. A. Huggins, *Solid State Ionics*, 86-88 (1996) 841.
17. Y. Zou and Y. Wang, *Nanoscale*, 3 (2011) 2615.
18. P. Poizot, S. Laruelle, S. Grugeon, L. Dupont, and J. M. Tarascon, *Science*, 407 (2000) 496.
19. D. Aurbach, B. Markovsky, I. Weissman, E. Levi, and Y. Ein-Eli, *Electrochimica Acta*, 45 (1999) 67.
20. A. Lasia, *Electrochemical Impedance Spectroscopy and its Applications*, Springer, (2014) New York, USA.
21. M. E. Orazem and B. Tribollet, *Electrochemical Impedance Spectroscopy*, John Wiley & Sons, (2008) Hoboken, USA.
22. C. Marino, A. Darwiche, N. Dupré, H. A. Wilhelm, B. Lestriez, H. Martinez, R. Dedryvère, W. Zhang, F. Ghamouss, D. Lemordant, and L. Monconduit, *The Journal of Physical Chemistry C*, 117 (2013) 19302.
23. S. S. Zhang, K. Xu, and T. R. Jow, *Electrochimica Acta*, 49 (2004) 1057.
24. E. Barsoukov, J. H. Kim, J. H. Kim, C. O. Yoon, and H. Lee, *Solid State Ionics*, 116 (1999) 249.
25. E. Barsoukov, *Solid State Ionics*, 161 (2003) 19.

26. Y. Wang, J. Qiu, Z. Yu, H. Ming, M. Li, S. Zhang, and Y. Yang, *Ceramics International*, 44 (2018) 1312.
27. Y. Liu, G. Zhou, K. Liu, and Y. Cui, *Acc. Chem. Res.*, 50 (2017) 2895.

© 2018 The Authors. Published by ESG ([www.electrochemsci.org](http://www.electrochemsci.org)). This article is an open access article distributed under the terms and conditions of the Creative Commons Attribution license (<http://creativecommons.org/licenses/by/4.0/>).